BB

ASITP

INSTITUTE OF THEORETICAL PHYSICS ACADEMIA SINICA

AS-ITP-95-19
June 1995

Incomplete Fusion-Fragmentation Model Agrees With Aladin Multifragmentation Data

CERN LIBRARIES, GENEVA
SCAN-9604032

SW 9615

Zheng Yu-Ming, Wang Fei
Sa Ben-Hao and Zhang Xiao-Ze

P.O.Box 2735, Beijing 100080, The People's Republic of China

Telefax : (86)-1-2562587 Telephone : 2568348

Telex : 22040 BAOAS CN Cable : 6158

INCOMPLETE FUSION-FRAGMENTATION MODEL AGREES WITH ALADIN MULTIFRAGMENTATION DATA

Zheng Yu-Ming[1,2], Wang Fei[2], Sa Ben-Hao[1,2,3] and Zhang Xiao-Ze[2]

1. CCAST (World Lab.),P.O.Box 8730,Beijing 100080.China.
2. China Institute of Atomic Energy,P.O.Box 275(18), Beijing 102413.China.[1]
3. Institute of Theoretical Physics, Academia Sinica, Beijing China.

Abstract

The incomplete fusion-fragmentation model is modified to confront with the ALADIN multifragmentation data of the projectile remnant in reaction of 600 MeV/nucleon Au bombarding with different targets. Since the incomplete fusion-fragmentation model includes both the dynamical formation and the statistical disassembly of hot nucleus, all of the ALADIN obserables can be reproduced quite well as if the model parameter concerning excitation energy is somewhat adjusted due to the mean multiplicity of intermediate mass fragment as a function of total bound charge.

PACS number(s): 25.70.Np

1 Introduction

The multifragmentation of hot nuclei and the Intermediate Mass Fragment (IMF) in energetic nucleus-nucleus collisions are one of the most widely investigated issue both experimentally[1-7] and theoretically[8-30]. Multifragmentation of hot nucleus is characterized by emission of more than two intermediate mass fragments. IMF stands for the fragment with charge number $3 \leq Z_f \leq 30$. IMF is difined for studying the on set of multifragmentation decay mode of hot nucleus, instead of charge (mass) number of referential fragment introduced in [27-30]. The theoretical studies of multifragmentation can be mainly cataloged into the following branches: the dynamical approach[14-16],the

[1]mailing address.

statistical model[8-13, 27], the percolation model[17-20] and the combination of statistical and dynamical calculations[21-26].

Although the dynamical simulation is very powerful in describing the space-time evolution of reaction system and the particle production etc., it is not able to reproduce the yield of IMFs. The statistical model, on the other hand, has had great successes in describing the various distributions (e.g. mass, charge and energy distributions) of fragments and the yield of IMFs. In fact, all of those successes could be regarded as the evidence of that the nuclear system has reached a certain state of thermal equilibrium. That fact is not commonly accepted, however, since the thermal equilibrium is one of the basic assumption of the statistical model. Whether the nuclear system approaches the thermal equilibrium during the later stages of intermediate energy nucleus-nucleus collisions, remains a debating subject anyways[31].

Recent published ALADIN data of correlations among the charges of fragments emitted from the projectile remnant in the reactions of 600 MeV/nucleon Au projectile on different targets[32-36] support stongly the establishment of the thermal equilibrium in the fragmenting nucleus (hot nucleus) before break-up. That has attracted, of course, great interest among theorists. Those correlations include the mean multiplicity of IMFs, the average charge of the largest fragment (Z_{max}), the ratio of charge moments (γ_2), the asymmetry of largest to second largest charge (a_{12}) and the three-body asymmetry parameter (a_{123}) as a function of the Z_{bound} (which is the sum of the charges of fragments with $Z_f \geq 2$). All the aforementioned correlations are almost independent on the targets[33-35], the bombarding energies[36] and the measured techniques[37]. That evidences the thermal equilibrium of fragmenting nucleus before break-up.

There are a lot of attempts to analyse ALADIN data with the statistical model or combination of dynamical and statistical calculations or the hybrid dynamical-percolation approach[38-41]. Since the presently available dynamical model do not allow for an unambiguous determination of the break-up condition of fragmenting nucleus and the excitation energy, which always extracted extremely high, the dynamical simulation is nothing to do with the reproducing of ALADIN data at the moment[35,42]. In Ref. 39 it was proved that if the input parameters of statistical calculations, i.e. the mass number and the excitation energy of fragmenting nucleus, were determined by adjusting them so as to reproduce the mean IMF multiplicity as a function of average Z_{bound}, the remains of ALADIN data could be well reproduced by the statistical model itself. A better way to reproduce the ALADIN data was then introduced in Refs. 35, 38, 40 and 41. That is the calculation which starts from dynamical simulation (internuclear cascade in Ref. 38, BUU in 35, 40 and 41) and turns into statistical or percolation calculation (Moscow version of Copenhagen model in Ref. 38, Berlin-Beijing model in Ref. 40 and percolation model in

Ref. 41) once the mass number and the excitation energy of fragmenting nucleus have been properly defined from the dynamical simulation. However, where it was required that one needs first to fit the correlation of $< M_{IMF} >$ vs. $< Z_{bound} >$ by adjusting the excitation energy (in Ref. 35 and 40) or the definition of source (in Ref. 38).

In this paper the proposed Incomplete Fusion-Fragmentation Model(IFFM)[22-23, 43-44], which has already had successes in describing the disassemply of hot nucleus in intermediate energy nuclear collisions, has been improved somewhat to confront with ALADIN data of the disassembly of projectile remnant (hot nucleus) in reaction of (600 MeV/nucleon)Au + Cu, for example. Since IFFM is a hybrid dynamical-statistical model, it is turned out that only if the model parameter concerning the excitation energy of fragmenting nucleus is adjusted a little bit due to the correlation of $< M_{IMF} >$ vs. $< Z_{bound} >$, the other observed correlations are all reproduced quite well.

2 Model description

The experimental systematics of the logitudinal momentum transfer[45] have already indecated that complete fusion gives way to incomplete fusion if the incident energy exceeds 8-10 MeV/nucleon. In the model it is assumed, therefore, the formation of hot nuclei in interniediate energy nucleus-nucleus collisions is a dynamical incomplete fusion process.

Experiments also show that the fragments close to the target are formed in the peripheral interaction and the low mass fragments in the more central collisions. That enlightens us to relying on the participant-spectator picture in describing the formation of hot nuclei. One might assume that the projectile remnant (one of the hot nuclei) is composed of a part of projectile nucleons locating outside of the overlopping region between the target and the projectile nuclei under given impact parameter. The target nucleons and the remains of projectile nucleons form the target remnant (another hot nucleus). The projectile nucleons located inside the overlopping region can be calculated as follows:

$$N_P(b) = \rho_0 \int dV \theta\{R_P - [x^2 + (b-y)^2 + z^2]^{1/2}\}\theta\{R_T - (x^2+y^2)^{1/2}\}, \qquad (1)$$

where ρ_0=0.16 fm^{-3} refers to the normal nuclear density, θ stands for the step function, R_p and R_t are, respectively, the radius of projectile and target nuclei and b is the impact parameter. If one assumes further that the ratio of the charge number to mass number of the projectile remnant is equal to the corresponding ratio of the projectile nucleus, as did in Ref.35 and 38, the mass and charge numbers of the projectile and target remnants(A_P, Z_P, A_T and Z_T) are then decided.

Since the incident energy is quite high in comparing with the energy of Fermi motion or the energy of nucleon interaction, it is reasonable to assume further that in the initial

reaction stage the projectile spectator nucleons (missing mass,$A_P^0 - N_P$, A_P^0 refers to the mass number of projectile nucleus) escape as a whole (projectile remnant) with beam velocity. The reaction energy Q can then be calculated in vertue of mass balance. From the energy and momentum conservations, the kinetic energy deposited in the reaction system (projectile and target remnants) can be derived as well. The sum of the deposited energy and the reaction energy is regarded as the available reaction energy of the system

$$E_{avai.} = \frac{N_P}{A_P^0}\frac{A_T^0}{A_T^0 + N_P}E_{in} + Q, \qquad (2)$$

where A_T^0 stands for the mass number of target nucleus, E_{in} refers to the incident energy.

Above available reaction energy is then shared among the projectile and target remnant nucleons with different weight parameters of f_P and $f_T(= 1 + (1 - f_P)\frac{A_P}{A_T})$, respectively. The projectile remnant takes a share of

$$E_P = f_P \frac{A_P}{A_P + A_T} E_{avai.}. \qquad (3)$$

The excitation energy of projectile remnant can then be assumed as

$$E_P^* = C_P * E_P, \qquad (4)$$

where C_P is the fractional factor describing the part of energy E_P which turns into excitation energy. Since a certain portion of E_P should go to the expansion and the preequilibrium emission, C_P is less than one. The excitation energy per nucleon is then

$$\epsilon_P^* = E_P^*/A_P. \qquad (5)$$

As usual, one assumes that after expansion the aforeformed projectile (target) remnant approaches to the freeze-out state, which is described as a sphere with radius parameter R_h (h=P or T) greater than r_0=1.18 fm. The R_h and $C_f^P = f_P * C_P$ are regarded as the model parameters.

The Berlin-Beijing model[10] is then used to describe the disassembly of the projectile remnant at freeze-out. In this model it was assumed that the projectile remnant (hot nucleus) disassembles promptly into a configuration described by a set of variables $\{N_c, N_n, \{A_i, Z_i\}_{i=1}^{N_c}, \{\vec{r}_i\}_1^{N_c}, \{\vec{p}_i\}_1^{N_c}, \{\epsilon_i\}_1^{N_c}, \{\vec{r}_j\}_1^{N_n}, \{\vec{p}_j\}_1^{N_n}\}$. Here N_c refers to the number of charged fragments including prompt protons. N_n stands for the number of prompt and evaporated neutrons. $\{A_i, Z_i\}_{i=1}^{N_c}$, $\{\vec{r}_i\}_1^{N_c}$,$\{\vec{p}_i\}_1^{N_c}$ and $\{\epsilon_i\}_1^{N_c}$ are the set of mass and charge numbers, position, momentum and internal excitation energy of charged fragments. $\{\vec{r}_j\}_1^{N_n}$ and $\{\vec{p}_j\}_1^{N_n}$ are the set of position and momentum of neutrons.

The configurations allowed by the mass, charge, momentum and energy conservations were assumed to conform to a distribution of canonical or microcanonical ensemble[10].

By the means of the Monte Carlo method and the corresponding Metropolis pass a large number of allowed configurations (10^6, say) were generated and the physical observables could then be claculated as a statistical average.

3 Results and comparing with data

In Table 1 are given the results of N_P, N_T, A_P, Z_P, $E_{avai.}$, E_P, E_P^* and ϵ_P^* from the calculation of IFFM. The impact parameters here are the same as those in Ref. 35, 40 and 41. It should be mentioned that the excitation energies per nucleon exhibited in Tab. 1 are the results from the adjustment to fit the observed correlation of $< M_{IMF} >$ vs. $< Z_{bound} >$. The corresponding parameter C_f^P ($=f_P * C_P = 0.1 * 0.57$) is equal to 0.057. What shows in Fig. 1 is the ϵ_P^* as a function of impact parameter b.

Fig. 2 shows the correlation of $< M_{IMF} >$ vs. $< Z_{bound} >$, where the open circles refer to the ALADIN data and the full squares stand for the results of the incomplete fusion-fragmentation model calculations (same labels are used in Fig. 3-7 as well). One learns from this figure that the mean multiplicity of IMF increases first with the decreasing of $< Z_{bound} >$ (i.e. with the strength of violence of collision) and then turns to decrease after reaching the maximum at $< Z_{bound} > \sim 40$. It evidences the coexistence of variety decay modes of hot nucleus and the turning over of decay modes from the pseudoevaporation (or/and pseudofission) mode to the multifragmentation mode and then to the vaporization mode[27-30,46].

The distribution of $< Z_{max} >$ vs. $< Z_{bound} >$ is shown in Fig. 3. Perfect agreement between the ALADIN data and the calculations can be seen here. Fig. 3 exhibites that the $< Z_{max} >$ decreases rapidly with the decreasing of $< Z_{bound} >$. It means that the charges are shared by more light fragments if the collision is more violent.

Fig.4 gives the asymmetry of two largest fragments

$$a_{12} = \frac{Z_{max} - Z_2}{Z_{max} + Z_2} \tag{6}$$

as a function of $< Z_{bound} >$, where Z_2 refers to the charge of the second largest fragment. The calculated results agree satisfactorily with data. What shown in the Fig. 5 is the same story for the second to the third largest fragments

$$a_{23} = \frac{Z_2 - Z_3}{Z_2 + Z_3}. \tag{7}$$

A quite good agreement is also obtained.

The result of three-body asymmetry

$$a_{123} = \frac{\sqrt{(Z_{max} - < Z >)^2 + (Z_2 - < Z >)^2 + (Z_3 - < Z >)^2)}}{\sqrt{6} < Z >} \tag{8}$$

is given in Fig. 6, where

$$< Z >= \frac{1}{3}(Z_{max} + Z_2 + Z_3). \tag{9}$$

It varies smoothly with $< Z_{bound} >$ and reproduces the correspoding ALADIN data very well.

γ_2, the ratio of charge moment, is defined as

$$\gamma_2 = \frac{\sigma_c^2}{< Z >_c^2} + 1 \tag{10}$$

and shown in Fig. 7. In above equation σ_c^2 is the variance of the charge distribution within the event and $< Z >_c^2$ is the mean charge of the event. γ_2 approaches to its lower limit of one when all fragments have same charge. That might be corresponding to the pseudoevaporation or the vaporization decay mode of the disassembly of hot nucleus. The mean value of γ_2 indecates the size of the charge fluctuations. Fig. 7 shows that the ALADIN data of γ_2 are reproduced nicely.

4 Discussion and conclusion

First of all it should be mentioned that the equation (3) exhibits the relation between the excitation energy of projectile remnant and its mass number. It is resulted from adjusting the model parameter (C_f^P) to reproduce the correlation of $< M_{IMF} >$ vs. $< Z_{bound} >$. We are pleased that the unified value of the $C_f^P = f_P * C_P = 0.1 * 0.57 = 0.057$ is fitted for all of the calculated projectile remnants. That is better in comparing with making adjustment for every projectile remnant as did in Ref. 38-40.

It should be pointed out that the C_P=0.57, defined as a part of the parameter C_f^P and refered to the fraction of the projectile remnant energy going into excitation energy, is somewhat less than corresponding ones ($\sim 0.6 - 0.8$) used in Ref. 22-23 and 43-44. That is reasonable since the incident energy here is larger and the hot nucleus considered is the projectile remnant. The factor of f_P=0.1 is close to the value of the rolling friction coefficient[47] in magnitude. This means that the process of the available reaction energy transfering into projectile remnant might be regarded as a result of rolling friction when projectile nucleus and target nucleus pass through each other. It is quite consistent with the participant-spectator picture adopted.

In summary, it is turned out that the IFFM is not only good for describing the various distribution of fragments in disassembly of hot nucleus but also good for reproducing the ALADIN multifragmentation data, even though the dynamic involved in the IFFM is quite simple. It is because that the statistics plays more important role than the dynamics for the description of the behaviours of the final fragments.

We thank W. Trautmann for supplying the ALADIN data. Thanks also go to D. H. E. Gross for help and discussion. The discussion with B-A. Li is acknowleged. This work is supported by the National Natural Science Foundation of China.

References

1. J. W. Harris et al., Nucl. Phys. **A471**,241c(1987).

2. R. Trockel et al., Phys. Rev. **C39**,729(1989).

3. B. Jakobsson et al., Nucl. Phys. **A509**,195(1990).

4. K. Hagel et al., Phys. Rev. Lett. **68**,2141(1992).

5. L. G. Moretto, D. N. Delis and G. J. Wozniak, Phys. Rev. Lett. **71**, 3935(1993).

6. V. Lips et al., Phys. Rev. Lett. **72**,1604(1994).

7. L. G. Moretto and G. J. Wozniak, Prog. Part. Nucl. Phys. **30**,135(1993).

8. G. Bertsch and P. J. Siemens, Phys. Lett.,**B126**,9(1983).

9. J. Randrup and S. E. Koonin, Nucl. Phys. **A356**,223(1981);
   S. E. Koonin and J. Randrup, Nucl. Phys. **A474**,173(1987);
   G. Fai and J. Randrup, Nucl. Phys. **A487**,397(1988).

10. Sa Ben-Hao and D. H. E. Gross, Nucl. Phys. **A437**,643(1985);
    Zhang Xiao-Ze, D. H. E. Gross, Xu Shu-Yan and Zheng Yu-Ming, Nucl. Phys. **A461**,641(1987);
    Zhang Xiao-Ze, D. H. E. Gross, Xu Shu-Yan and Zheng Yu-Ming, Nucl. Phys. **A461**,668(1987);
    Y. M. Zheng, S. Y. Xu, X. Z. Zhang and D. H. E. Gross, Chinese Physics **10**,146(1990).

11. J. P. Bondorf, R. Donangelo, I. N. Mishustin, C. J. Pethick, H. Schulz and K. Sneppen, Nucl. Phys. **A443**,321(1985);
    J. P. Bondorf, R. Donangelo, I. N. Mishustin and H. Schulz, Nucl. Phys. **A444**,460(1985);
    H. W. Barz J. P. Bondorf, R. Donangelo, I. N. Mishustin and H. Schulz, Nucl. Phys. **A448**,753(1986).

12. W. A. Friedman and W. G. Lynch, Phys. Rev. **C28**,16(1983).

13. R. J. Charity et al., Nucl. Phys. **A483**,371(1988).

14. G. F. Bertsch and S. Das Gupta, Phys. Rep. **160**,189(1988).

15. J. Aichelin, Phys. Rep.,**202**,233(1991).

16. Zheng Yu-Ming, Sa Ben-Hao and Zhang Xiao-Ze, Chinese Phys. Lett.,**6**, 117(1989);
    L. De Paula, J. Nemeth, B-H. Sa, S. Leray, C. Ngo, H. Ngo, S. R. Souza and Y. M. Zheng, Phys. Lett. **B251**,251(1991).

17. W. Bauer, D. R. Dean, U. Mosel and V. Post, Phys. Lett. **B150**,53(1985);
    W. Bauer, Phys. Rev. **C38**,1297(1988);
    W. Bauer et al., Ann. Rev. Nucl. Sci. **42**,77(1992).

18. X. Campi, J. Phys. A: Math. Gen. **19**,L917(1986); Phys. Lett. **B208**,351(1988);
    J. Desbois, Nucl. Phys. **A466**,724(1987).

19. T. Biro, J. Knoll and J. Richert, Nucl. Phys. **A459**,692(1986).

20. H. Ngô, C. Ngô, F. Ighezou, J. Desbois, S. Leray and Y. M. Zheng, Z. Phys. **A337**,18(1990).

21. K. Sneppen and L. Vinet, Nucl. Phys. **A480**,342(1988).

22. Sa Ben-Hao, Zheng Yu-Ming and Zhang Xiao-Ze, Phys. Rev. **C40**,2680 (1989).

23. Zheng Yu-Ming, Chih Ta-Hai, Li Wen-Xin, Zhang Xiao-Ze and Sa Ben-Hao, Chinese J. Nucl. Phys. **14**,116(1992).

24. A. S. Botvina, A. S. Iljinov and I. N. Mishustin, Nucl. Phys. **A507**,649(1990).

25. S. Leray, C. Ngô, M. E. Spina, B. Remaud and F. Sebille, Nucl. Phys.**A511**,414(1990).

26. M. Colonna, P. Roussel-Chomaz, N. Colonna, M. Di Toro, L. G. Moretto and G. J. Wozniak, Phys. Lett. **B283**,180(1992).

27. Y. M. Zheng, H. Massmann, S. Y. Xu, D. H. E. Gross, X. Z. Zhang, Z. Q. Lu and B. H. Sa, Phys. Lett. **B194**,183(1987).

28. D. H. E. Gross, Zheng Yu-Ming and H. Massmann, Phys. Lett. **B200**,397(1988).

29. Sa Ben-Hao, Zheng Yu-Ming and Zhang Xiao-Ze, Int. J. Mod. Phys. **A5**,843(1990).

30. Sa Ben-Hao, Zheng Yu-Ming and Zhang Xiao-Ze, Nucl. Phys. **A509**, 499(1990).

31. Sa Ben-Hao, Wang Rui-Hong, Zhang Xiao-Ze, Zheng Yu-Ming and Lu Zhong-Dao. Phys. Rev. **C50**.2614(1994).

32. C. A. Ogilvie et al., Phys. Rev. Lett. **67**.1214(1991).

33. J. Hubele et al., Z. Phys. **A340**.263(1991).

34. J. Hubele et al., Phys. Rev. **C46**,R1577(1992).

35. P. Kreutz et al., Nucl. Phys. **A556**,672(1993).

36. W. Trautmann et al., GSI preprint 93-76 (1993); also GSI 05-94.

37. P. L. Jain, G. Singh and A. Mukhopadhyay, Phys. Rev. **C50**,1085(1994).

38. A. S. Botvina and I. N. Mishustin, Phys. Lett. **B294**,23(1992).

39. H. W. Barz, W. Bauer, J. P. Bondorf, A. S. Botvina, R. Donangelo, H. Schulz and K. Sneppen,Nucl. Phys. **A561**,466(1993).

40. Bao-An Li, A. R. DeAngelis and D. H. E. Gross, Phys. Lett. **B303**, 225(1993).

41. Y. M. Zheng, J. Richert and P. Wagner, Chinese J. Nucl. Phys. **17**,No.3(1995).

42. M. B. Tsang et al., Phys. Rev. Lett. **71**(1993)1502.

43. Chih Ta-Hai, Sa Ben-Hao, Zhang Xiao-Ze and Zheng Yu-Ming, Phys. Rev. **C42**,2187(1990).

44. Li Wen-Xin et al., Phys. Rev. **C48**.628(1993).

45. V. Viola et al., Phys. Rev. **C26**,178(1982);
Y. Chan et al., Phys. Rev.,**C27**,447(1983).

46. Sa Ben-Hao, Nucl. Phys. **A499**,480(1989).

47. H. J. Gray & Alan Isaacs, A New Dictionary of Physics, Longman, 1975.

Figure Captions

Fig.1 The mass number and the excitation energy of projectile remnants as a function of impact parameter.

Fig.2 Correlation between the average multiplicity of IMF (M_{IMF}) and the average total charge bounded in fragments with charge number $Z_f \geq 2$. Open circles : the ALADIN data of the disassembly of projectile remnant in the reaction (600 MeV/nucleon)Au + Cu. Full squares: results of IFFM.

Fig.3 The same as Fig.2 but for the correlation between $< Z_{max} >$ and $< Z_{bound} >$.

Fig.4 The same as Fig.2 but for the correlation between the asymmetry of two largest fragments and the $< Z_{bound} >$.

Fig.5 The same as Fig.2 but for the correlation between the asymmetry of second and third largest fragments and the $< Z_{bound} >$.

Fig.6 The same as Fig.2 but for the correlation between the three-body asymmetry and the $< Z_{bound} >$.

Fig.7 The same as Fig.2 but for the correlation between the ratio of charge moments,γ_2,and the $< Z_{bound} >$.

Table Captions

TABLE 1. The characteristics of projectile remnant in reaction (600 MeV/nucleon)Au + Cu calculated from the Incomplete Fusion-Fragmentation Model

b (fm)	N_T	N_P	A_P	Z_P	$E_{avai.}$ (GeV)	E_P (MeV)	E_P^* (MeV)	ϵ_P^* (MeV/nucleon)
1	63	130	67	27	25.45	655.8	373.8	5.58
2	63	123	74	30	24.99	711.4	405.5	5.48
3	63	108	89	36	23.85	816.3	465.3	5.23
4	60	90	107	43	22.29	917.3	523.0	4.90
5	50	72	125	50	20.23	972.8	554.5	4.44
6	40	54	143	57	17.52	963.4	549.1	3.84
7	29	38	159	64	14.28	873.4	497.8	3.13
8	18	24	173	69	10.47	696.7	402.7	2.33
9	10	13	184	74	64.90	459.3	261.8	1.42
10	4	5	192	77	27.85	205.6	117.2	0.61

Fig.2

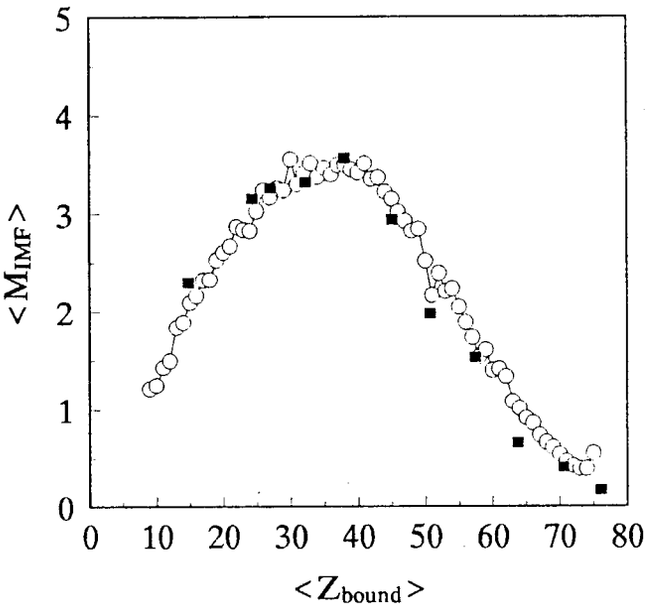
5
4
3
2
1
0
0 10 20 30 40 50 60 70 80
<M_IMF>
<Z_bound>

Fig.1

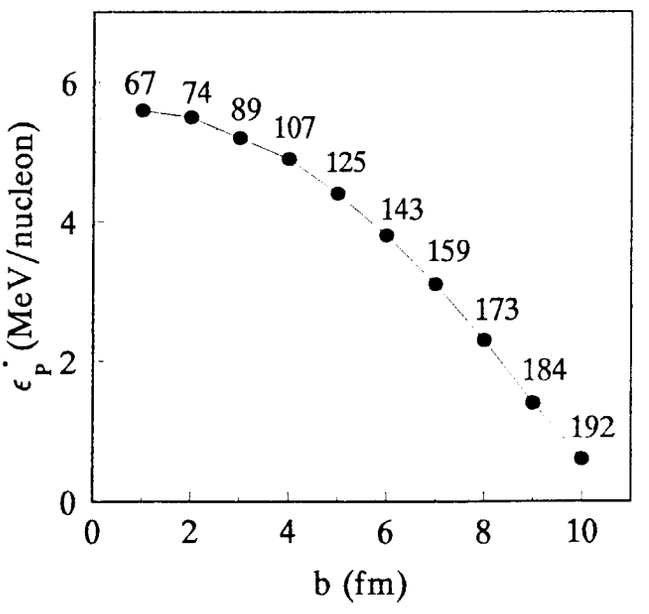
67
74
89
107
125
143
159
173
184
192
6
4
2
0
0 2 4 6 8 10
ε_P (MeV/nucleon)
b (fm)

Fig.4

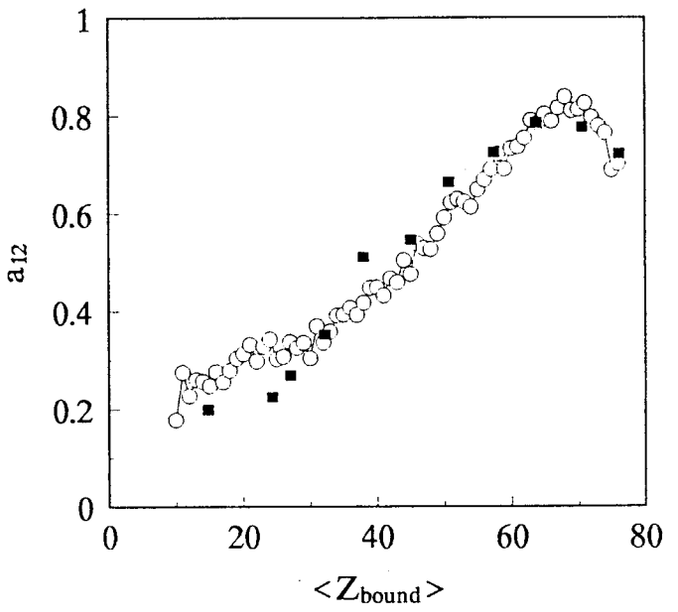

Fig.3

Fig.6

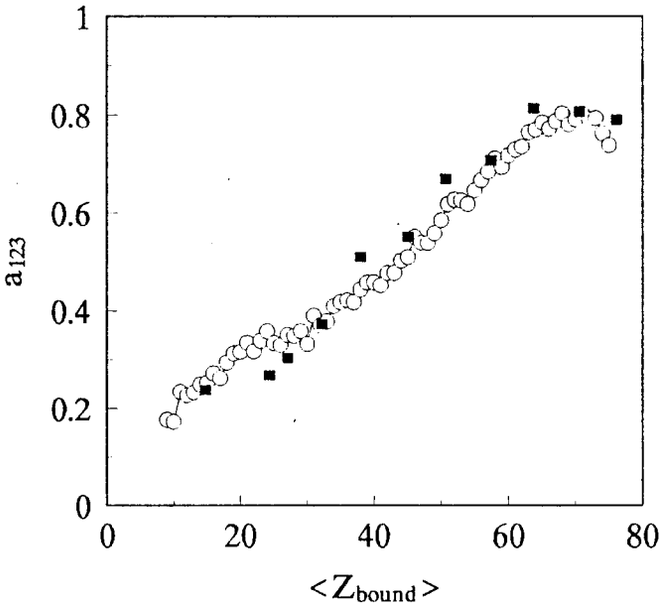
1
0.8
0.6
0.4
0.2
0
0
20
40
60
80
a123
<Zbound>
<Zbound>

Fig.5

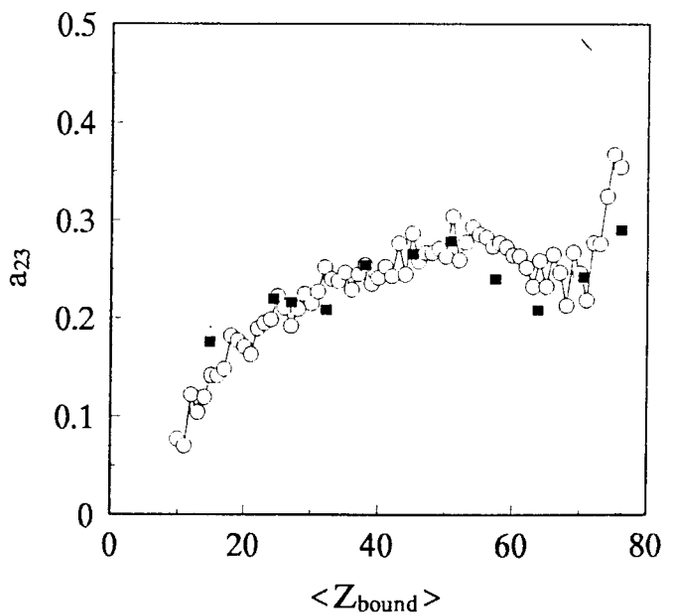
0.5
0.4
0.3
0.2
0.1
0
0
20
40
60
80
a23
<Zbound>
<Zbound>

Fig.7